

# Voids in the Cosmic Web as a probe of dark energy

B. Novosyadlyj, M. Tsizh

Astronomical Observatory of Ivan Franko National University of Lviv,  
Kyryla i Methodia Str., 8, Lviv, 79005, Ukraine

Received January 16, 2017

The formation of large voids in the Cosmic Web from the initial adiabatic cosmological perturbations of space-time metric, density and velocity of matter is investigated in cosmological model with the dynamical dark energy accelerating expansion of the Universe. It is shown that the negative density perturbations with the initial radius about 50 Mpc in comoving to the cosmological background coordinates and the amplitude corresponding to the r.m.s. temperature fluctuations of the cosmic microwave background lead to the formation of voids with the density contrast up to  $-0.9$ , maximal peculiar velocity about 400 km/s and the radius close to the initial one. An important feature of voids formation from the analyzed initial amplitudes and profiles is establishing of the surrounding overdensity shell. We have shown that ratio of the peculiar velocity in units of the Hubble flow to the density contrast in the central part of void does not depend or depends weakly on the distance from center of the void. It is shown also that this ratio is sensitive to the values of dark energy parameters and can be used for finding them on basis of the observational data on mass density and peculiar velocities of galaxies in the voids.

**Key words:** *cosmological perturbations, dark energy, large scale structure of the Universe, voids, Cosmic Web*

**PACS:** *95.36.+x, 98.80.-k*

## 1. Introduction

The cosmological constant, which has been introduced into general relativity one hundred years ago by Albert Einstein [1], played an important role in development of the theory of structure and evolution of the Universe. At the end of XXth century two research teams, SuperNova Cosmology Project and High-z SuperNova Search, have performed the cosmological test “magnitude – redshift” for type Ia supernovae and obtained the secure observational evidence (at  $3\sigma$  C.L.) for non-zero positive value of the cosmological constant [2–4] and accelerated expansion of the Universe as a consequence. Since the cosmological constant has no consistent physical interpretation, other essences have been proposed to explain the accelerated expansion of the Universe. They have been commonly referred to as the “dark energy” [5]. Among them the most elaborated ones are the scalar field models of dark energy [6–9]. In the “world ocean” of different variants of such models one can distinguish a few “main streams” like quintessential, phantom, quintom and others. Accurate observations and new crucial tests are needed to discriminate between these candidates and decide which one fills our Universe. In numerous papers of the last decade it was shown that the large voids in large scale structure of the Universe are excellent laboratories for this [10–20]. Here we show that the data on dynamical structure of the voids, positions, number densities and peculiar velocities of the galaxies at central parts of the voids are sensitive to the parameters of dark energy.

## 2. Voids in Cosmic Web

The space distribution of luminous matter, which is collected in galaxies, forms the large scale structure of the Universe. Its elements – clusters, superclusters, walls, sheets, filaments, nodes and voids – form the complex geometrical and topological system which is dubbed sometimes the Cosmic Web [21].

It emerged from the quantum fluctuations of space-time metric generated in the early universe and stretched to the cosmic scale by inflation. Its formation in the expanding Universe is a long history of action of the forces of self-gravitation of luminous matter, gravity of dark matter and “anti-gravity” of dark energy on large scales. The complexity of the structure requires the sophisticated methods of analysis. Methods of complex systems analysis which have been developed recently [22–24] may be helpful for understanding of the hidden patterns of such structures. In this section we will walk through the history of study of voids and review shortly the most prominent recent works in this field.

In 1978 S. Gregory and A. Thompson [25] and independently of them M. Joeveer, J. Einasto and E. Tago [26] noticed while studying superclusters that there are areas in the galaxy field where the galaxy density is significantly lower than the average one (Joeveer referred to them as to “holes” in the distribution). Very soon it became obvious that these holes – or, as we call them now, cosmic voids – are very important in the matter distribution and its evolution. In the 1980s devoted to the cosmic voids papers by renowned cosmologists appeared (by Zeldovich [27] and Silk [28]). They have shown that the progenitors of voids were primordial adiabatic cosmological perturbations, the same as for the clusters and galaxies, but with the opposite sign. In the same period, first papers describing analytically the evolution of voids with certain profile were written by Sato [29] and Maeda [30]. The analytic solutions of the evolution equations for voids predicted already some important features of the voids, in particular, their expansion during evolution, in contrary to the collapse of halos, and formation of the overdensity shell, the same as we observe in our numerical solutions. Another important feature, tendency to sphericity of the voids, was shown by M. Fujimoto [31] and V. Icke [32].

Unlike the clusters and galaxies, cosmic voids are much harder to track, as they are underdense and hence un luminous. So it is not surprising that the N-body cosmological simulation of the large scale distribution became a powerful tool in studying voids, as they have observational fullness of the void population in comparison to the real distribution. The first papers describing the voids in the numerical simulation were written in 1984 [33].

Soon after that, the amount of data on large scale structure of the Universe increased enough, so the properties of cosmic voids began being studied statistically. Already in 1985 Vettolani and colleagues give statistics on the volume distribution of 200 real voids [34]. The latest and largest galaxy catalogue, on which the void-finding algorithm was imposed, is SDSS DR12. Q. Mao and colleagues have found more than 10 000 voids there in the redshift range  $0.1 < z < 0.7$  [35].

In the late 1980s the papers discussing lack of voids in the Ly-alpha forest began to emerge ([37], [36]). Due to the faintness of young galaxies, the discovery of voids at  $z > 1$  came only in 1991 [38]. The modern searches for early voids in cosmological simulations were carried in [39] and in observable data in [40], highlighting, probably, the most distant observable voids at  $z = 5.7$  in the spatial distributions of the Lyman-alpha emitters.

Nevertheless, many of secrets of the voids’ nature were discovered in distributions obtained from numerical simulations, including the void universal density profile [18]. The  $\Lambda$ CDM cosmology simulation with probably the largest number of voids was done in 2004, where in total 80 000 voids were found in the simulated distribution [41]. Another interesting work was written by S. Gottlober and colleagues [42], where they studied the mass distribution in voids, halos in the void, the void mass function and its dependence on radius using results of the high-resolution N-body simulation. With the development of such simulations it became possible to track the evolution of voids in such simulated universes. The authors of [43–45] studied the changes of profiles and sizes of the void population with  $z$ . Modern results on voids from N-body simulations are given in [46, 47].

The influence of surroundings on the formation of voids as well as their hierarchical structure became clear in 1990s and early 2000s. Being underdense fragile structures, the voids can be crushed by the infall of outer regions (void collapse) or merge into the larger void. The first paper describing the void clustering was written in 1994 by S. Haque-Copilah and D. Basu [48], the interaction of two voids was considered in 1993 by J. Dubinski [49]. In 2003-2004 R. van de Weygaert and R. Sheth wrote several papers [50, 51], summing up studies of the void hierarchy problem. In the latter paper authors managed to formulate the excursion set formalism of void formation and evolution in the manner it was previously done for halos (see also [15] and [14]). They give clear classification of the types of voids and their density depending on their neighborhood (void-in-clouds and void-in-voids). They also sum up studied at that time general properties of voids.

Starting from the paper [52] the void statistics is used for constraining of different cosmological parameters [17], probing of dark energy [11, 12, 18], testing of modified gravity [10, 13, 14, 16]. After L. Amendola and colleagues computed the weak gravitational lensing by voids [53] it became possible to find the constraints on cosmological parameters from the influence of this lensing on the cosmic microwave background (CMB) [54] (an example of how voids can be studied through the gravitational lensing produced by them is given in [55]). Another important cosmological test, the Alcock-Paczynski test [56], was predicted and tested in the N-body simulation by Lavaux [57] and then confirmed in the observational data by Sutter and team [58]. They used the stacked cosmic voids identified in the SDSS DR7 and DR10 and measured their ellipticity. The essence of this test is in the statistical study of the form of large scale structures. If one uses the correct cosmology, the relation of sizes along and transverse to the line of sight shows no dependence on  $z$ . The results confirmed that the dark energy has no alternatives, but they do not distinguish between the models of dark energy.

In 2008 M. Neyrinck published [59] the algorithm for finding the voids in 3D-galaxy distribution called ZOnes Bordering On Voidness (ZOBOV). This algorithm uses the Voronoi tessellation to divide the volume into regions with some averaged density. The center of each Voronoi cell is one galaxy. After that it applies the watershed landform to the obtained 3D density map to find the edges of voids. ZOBOV algorithm is claimed to be free of parameters and assumptions about the shapes of expected voids. It became really popular among the researchers and they now usually use ZOBOV or its modifications (like, for example, project VIDE [60]) to find voids in the cosmological simulation data or real galaxy catalogs.

Despite the far from spherical shape of the walls of the most voids and the influence of surroundings, study of the evolution of a spherical isolated void supplies us with the valuable hints in describing main physical characteristics of the void, including sometimes astonishingly accurate quantitative guidelines [47]. The universal density profile of a spherical void has been proposed by N. Hamaus, P. Sutter and B. Wandelt [61]. The profile has 4 parameters characterizing the size and steepness of the void and its overdensity shell. The authors argue that there is some relation between the form of void and its size and hence the parameters are not independent. They show possible dependences that may exist. This work causes the wide discussion, for example, experts are disputing whether the parameters of stacked voids profile would be the same [62] or different [63] for the simulation and real galaxy distribution.

Finally, we would like to emphasize the role of voids as a probe of dark energy. B. Li [66] have shown that voids can be used to rule out observationally or distinguish between coupled scalar field models of dark energy. Voids are also sensitive to the massive gravity dark energy models [67]. Usually, the shape of voids is studied statistically to constrain parameters of dark energy [11, 12, 68]. Also, with universal density profile one can improve the Alcock-Paczynski test by specifying the galaxies' redshift distortion and recovering the shape of voids, which, again, help to constrain the dark energy parameters [17, 18]. Our work is an essential complement to these ones, allowing to follow the evolution of single void with all its features.

### 3. Spherical voids: the dependence of velocity to density perturbations ratio on dark energy parameters

In our previous papers [19, 20] we have analysed the formation of single spherical voids in the three-component medium (matter, radiation and dark energy) from the early epoch up to the current one. We described each component in the hydrodynamical approximation. The model of minimally coupled dynamical dark energy had three free parameters: the energy density in units of the critical one at current epoch<sup>1</sup>  $\Omega_{de} \equiv 8\pi G\varepsilon_{de}^0/3H_0^2$ , the equation of state parameter  $w_{de} \equiv p_{de}/\varepsilon_{de}$  and the squared effective sound speed  $c_s^2 \equiv \delta p_{de}/\delta\varepsilon_{de}$  in the rest frame of dark energy. We assumed that the last two parameters are constant. Here and below we use the units in which the speed of light in vacuum  $c = 1$ , all velocities are in the units of speed of light.

We have shown in [20] how the spherical cosmological perturbation evolves to form the void with approximately universal density and velocity profiles. Here we will show that the ratio of matter velocity

---

<sup>1</sup>Hereafter the values of variables at the current epoch are marked by the upper or lower index 0.

and density perturbations, which can in principle be measured, is sensitive to the values of main parameters of the dynamical dark energy. This ratio does not depend on the initial amplitude at the linear stage of evolution. Since the large voids in the spatial distribution of matter, traced by galaxies, are now at quasi-linear stage of their evolution, the dependence on initial amplitude is predictable and can be estimated from the numerical calculations or N-body simulations. On the other hand, the large voids in the Cosmic Web are almost spherical, so the dependence of this ratio on the profile of initial perturbation and the impact of environment can be also removed, at least for the central part of voids. In this work we only outline the key dependences for the new possible test and leave the mentioned here important aspects of its implementation for future papers.

### 3.1. Assumptions and equations

Let us consider the evolution of spherical adiabatic cosmological perturbations in the Universe filled with the matter, dynamical dark energy and relativistic component. The last one is important in the early Universe when we set the initial conditions following from the observational data on the CMB anisotropy (see for details [20]). We present the space-time metric in the region of a perturbation in the Newtonian gauge as follows:

$$ds^2 = e^{v(t,r)} dt^2 - a^2(t) e^{-v(t,r)} [dr^2 + r^2(d\theta^2 + \sin^2\theta d\varphi^2)], \quad (3.1)$$

where  $t$  is the cosmological time,  $r$  is the radial coordinate comoving to the unperturbed background,  $\theta$  and  $\varphi$  are the polar and azimuth angles in the spherical 3D coordinates and  $a(t)$  is the scale factor of cosmological background. The function  $v(t, r)$  is the metric perturbation caused by the local density perturbation of all components. At distances larger than the radius of void,  $r \gg r_v$ ,  $v(t, r) \rightarrow 0$  and the metric (3.1) becomes the Friedmann-Lemaitre-Robertson-Walker (FLRW) one. The time dependence of the scale factor is determined by the Friedmann equation

$$H^2 \equiv \left( \frac{d \ln a}{dt} \right)^2 = H_0^2 (\Omega_{rel} a^{-4} + \Omega_m a^{-3} + \Omega_k a^{-2} + \Omega_{de} a^{-3(1+w_{de})}). \quad (3.2)$$

In the computations below we set the Hubble constant  $H_0$  to be 70 km/s · Mpc, this value lies between the “global” ( $67.8 \pm 0.9$  km/s · Mpc [64]) and “local” ( $73.24 \pm 0.74$  km/s · Mpc [65]) measurements. The spatial curvature, as the Planck 2015 results show, is very close to zero with  $|\Omega_k| < 0.005$ , that is why in the most of computations we will put it equal zero.

In the spherical perturbed region the contravariant components of 4-velocity of any component  $u_N^i \equiv dx^i/ds$  in the metric (3.1) are

$$u_N^i(t, r) = \left\{ \frac{e^{-v/2}}{\sqrt{1-v_N^2}}, \frac{e^{v/2} v_N}{a \sqrt{1-v_N^2}}, 0, 0 \right\}, \quad (3.3)$$

where the radial component of 3-velocity  $v_N$  is defined as the ratio of proper space interval to proper time interval at the distance  $r$  from center of the void:  $v_N(t, r) = e^{-v} dr/dt$  (in units of speed of light). In the  $v_N \ll 1$  approximation the components of energy-momentum tensor of any component  $T_{j(N)}^i = (\varepsilon_N + p_N) u_N^i(t, r) u_{j(N)} - \delta_j^i p_N$  to the second order of smallness are as follows:

$$T_{0(N)}^0 = \varepsilon_N + (\varepsilon_N + p_N) v_N^2, T_{0(N)}^1 = (\varepsilon_N + p_N) \frac{e^v}{a} v_N, T_{1(N)}^1 = -p_N - (\varepsilon_N + p_N) v_N^2, T_{2(N)}^2 = T_{3(N)}^3 = p_N. \quad (3.4)$$

We present the energy density of every component as sum of the mean (or background) value  $\bar{\varepsilon}_N(t)$  and the local perturbation:  $\varepsilon_N(t, r) = \bar{\varepsilon}_N(t)(1 + \delta_N(t, r))$ , where  $\delta_N$  denotes the relative density perturbation. The pressure of every component in the void is presented as  $p_N(t, r) = w_N \bar{\varepsilon}_N(t) + \delta p_N(t, r)$ . For the scalar field models of dark energy the non-adiabatic component of pressure perturbation  $\delta p_N(t, r)$  is important (see Appendix A in [69] and references therein). Taking it into account, the pressure perturbation of any component in the generalised form can be presented as

$$\delta p_N(t, r) = c_{s(N)}^2 \bar{\varepsilon}_N \delta_N(t, r) - 3 \bar{\varepsilon}_N a H (1 + w_N) (c_{s(N)}^2 - w_N) \int v_N(t, r) dr.$$

For the relativistic component with  $c_{s(rel)}^2 = w_{rel} = 1/3$  and the matter one with  $c_{s(m)}^2 = w_m = 0$  the non-adiabatic term disappears.

Therefore, in the metric (3.1) the Einstein equation  $G_0^0 = \kappa T_0^0$  and the conservation law  $T_{i;j}^j = 0$  give us the system of equations for metric, density and velocity perturbations of the matter, dark energy and relativistic components in the expanding Universe with dynamical dark energy:

$$v'' + \frac{2}{r}v' - 3a^2H^2(a\dot{v} + v) = 3H_0^2(\Omega_m a^{-1}\delta_m + \Omega_{rel} a^{-2}\delta_{rel} + \Omega_{de} a^{-(1+3w)}\delta_{de}), \quad (3.5)$$

$$\begin{aligned} \dot{\delta}_N + \frac{3}{a}(c_s^2 - w_N)\delta_N + (1 + w_N) \left[ \frac{v'_N}{a^2H} + \frac{2v_N}{a^2Hr} - 9H(c_s^2 - w_N) \int v_N dr - \frac{3}{2}\dot{v} \right] \\ + (1 + c_s^2) \left[ \frac{\delta'_N v_N}{a^2H} + \frac{\delta_N}{a^2H} \left( v'_N + \frac{2}{r}v_N \right) - \frac{3}{2}\delta_N \dot{v} \right] = 0, \end{aligned} \quad (3.6)$$

$$\begin{aligned} \dot{v}_N + (1 - 3c_s^2) \frac{v_N}{a} + \frac{c_s^2 \delta'_N}{a^2H(1 + w_N)} + \left( 1 + \frac{1 + c_s^2}{1 + w_N} \delta_N \right) \frac{2v_N}{a^2H} \left( v'_N + \frac{v_N}{r} \right) + \\ \frac{v'}{2a^2H} + \frac{1 + c_s^2}{1 + w_N} \left[ \dot{\delta}_N v_N + \delta_N \dot{v}_N + (1 - 3w_N) \frac{\delta_N}{a} v_N + \frac{v' \delta_N}{2a^2H} \right] = 0. \end{aligned} \quad (3.7)$$

We have rewritten the derivatives with respect to the time  $\frac{d}{dt}$  as the derivatives with respect to the scale factor  $\frac{d}{dt} = aH \frac{d}{da}$  and denoted them as  $(\dot{\phantom{x}})$ . The derivatives with respect to the radial coordinate  $\frac{d}{dr}$  are denoted here as  $(\prime)$ . So, the system (3.5)-(3.7) for 7 unknown functions must be integrated with respect to the scale factor  $a$  together with the algebraic equation (3.2). To integrate them the initial conditions must be set.

### 3.2. Initial conditions

We set the initial conditions in the early epoch when the amplitudes of perturbations are small ( $\delta_N(a, r) \ll 1$ ,  $v_N(a, r) \ll 1$  and  $v(a, r) \ll 1$ ) and the scale of perturbation is essentially larger than the particle horizon. For the radiation dominated epoch we obtain from the superhorizon asymptotic for the growth mode of cosmological perturbations the relations between initial amplitudes:

$$\frac{4}{3}\delta_m(a_{init}, r) = \frac{4}{3} \frac{\delta_{de}(a_{init}, r)}{1 + w_{de}} = \delta_{rel}(a_{init}, r) = -v(a_{init}, r), \quad (3.8)$$

$$v_m(a_{init}, r) = v_{de}(a_{init}, r) = v_{rel}(a_{init}, r) = -\frac{v'(a_{init}, r)}{4a_{init}H(a_{init})}. \quad (3.9)$$

We set the local initial perturbation as a bell-like hill for the metric function  $v(a_{init}, r) = C(1 - \kappa^2 r^2)e^{-r^2/r_d^2}$  and an inverted bell-like profile for the density, where a free constant  $C$  may be linked to the amplitude of the power spectrum of curvature perturbations measured at the last scattering surface of relic thermal radiation (see for details [20, 69]). We put here  $C = 3 \cdot 10^{-4}$ . We specify other parameters of this profile, which define the initial size and the slope of wall, as follows:  $\kappa^{-1} = 50$  Mpc,  $r_d = 25$  Mpc.

The initial profiles of matter density perturbations  $\delta_m(a_{init}, r)$ ,  $\delta_{de}(a_{init}, r)$ , velocity  $v_m(a_{init}, r) = v_{de}(a_{init}, r) = v_{rel}(a_{init}, r)$  and gravitational potential  $v(a_{init}, r)$  are presented in the left panel of Fig. 1.

### 3.3. Results and discussions

For numerical integration of the system of equations (3.5)-(3.7) with initial conditions (3.8)-(3.9), we have used the code *npdes.f2*. The results are presented in the central panel of Fig. 1. It illustrates how the initial spherical matter density perturbation in form of the inverted bell-like underdense profile with initial amplitude  $\delta_m(a_{init}, r = 0) = -2.25 \cdot 10^{-4}$  and radius  $r_v \equiv \kappa^{-1} = 50$  Mpc evolves to the spherical void with density contrast  $\delta_m(a = 1, r = 0) \approx -0.9$  and comoving radius  $r_{\delta=0} \approx 42$  Mpc. The matter, which is

<sup>2</sup><http://194.44.198.6/~novos/npdes.tar.gz>; the method of integration described in [20].

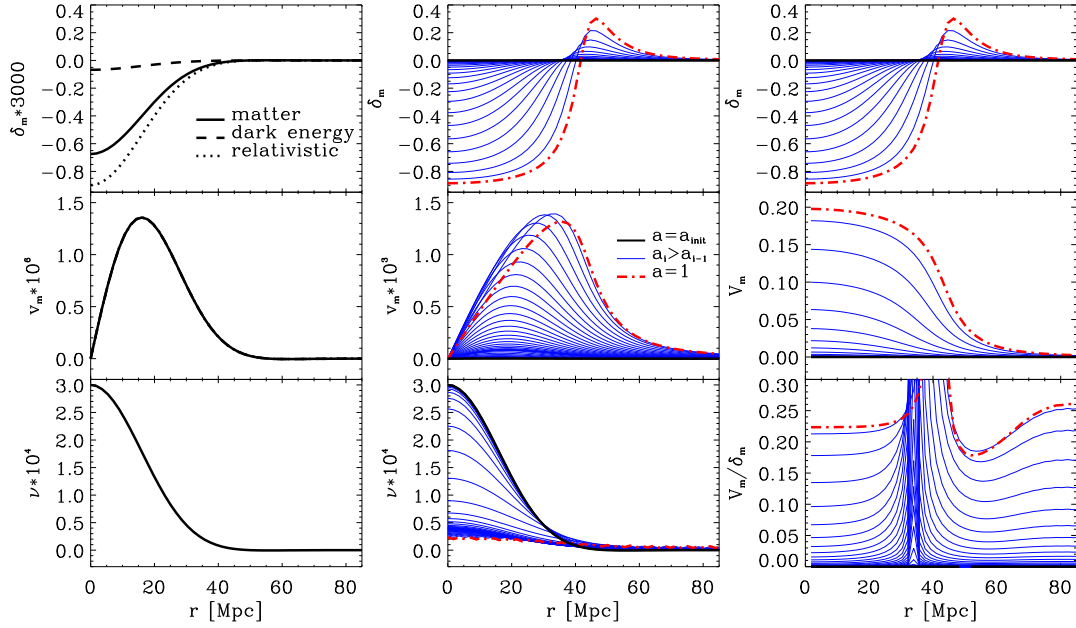


**Figure 1.** Formation of the void from the cosmological spherical perturbation. Left column: the initial profiles of density and velocity perturbations of matter and gravitational potential. Central column: evolution of the density  $\delta_m$  and velocity  $v_m$  perturbations of matter and gravitational potential  $\nu$  from the initial profiles (thick black lines) to the final one at  $a = 1$  (thick dashed red lines). Right column: evolution of the density perturbation (top), the velocity in units of the Hubble flow  $V_m$  (middle) and the ratio  $V_m/|\delta_m|$  (bottom).

flowing from the central part of void outwards, is collected in its peripheral part, forming an overdense shell and reducing somewhat the size of void in the comoving coordinates.

Maximum of the peculiar velocity of matter is reached at  $6/7$  of the void final radius and is  $v_m(1, r_{maxv}) \approx 400$  km/s. The value of Hubble flow  $V_H = H_0 r$  at this distance from center of the void ( $r_{maxv} \approx 36$  Mpc) equals approximately 2520 km/s. The ratio  $v_m/V_H$  is  $\approx 0.15$ . In the middle panel of right column of Fig. 1 we present the peculiar velocity of matter in units of the Hubble flow:  $V_m \equiv v_m(r)/H_0 r$ . It has the bell-like form with maximum  $\approx 0.20$  in this special case. Comparing the inverted bell-like form of  $\delta_m(r)$  (top panel) with the bell-like form of  $V_m(r)$  one suggests that their ratio does not depend on radius in the central part of void. Curves in the bottom panel support this assumption:  $V_m(r)/\delta_m(r) \approx const$  at any  $a$  for  $0 \leq r \leq 0.5r_{\delta=0}$ . Let us analyse how this ratio depends on the dark energy parameters.

The dark energy impacts the evolution of matter density and velocity perturbations in two ways. The first one is realised via the rate of expansion of the Universe: the equations (3.6)-(3.7) for matter density and velocity perturbations contain the function  $H(a)$ , eq. (3.2), which depends on  $\Omega_{de}$  and  $w_{de}$ . The second way consists in impact of the density perturbations of dark energy on the evolution of matter density and velocity perturbations via the gravitational potential  $\nu$ , eq. (3.5). The evolution of dark energy density and velocity perturbations, eqs. (3.6)-(3.7), depends on  $\Omega_{de}$ ,  $w_{de}$  and  $c_s^2$ . To estimate the level of impact of dark energy on the ratio  $V_m(r)/|\delta_m(r)|$  for dark matter we integrate the system of eqs. (3.5)-(3.7) in the simplified version ( $\nu$ ,  $\delta_m$ ,  $v_m$ ,  $\delta_{rel}$ ,  $v_{rel}$ ) and the full version ( $\nu$ ,  $\delta_m$ ,  $v_m$ ,  $\delta_{de}$ ,  $v_{de}$ ,  $\delta_{rel}$ ,  $v_{rel}$ ), without and with the density and velocity perturbations of dark energy.

In Fig. 2 we show the dependences of ratio  $V_m(r)/|\delta_m(r)|$  on scale factor  $a$  when the dark energy perturbations have not been taken into account. Here and below all dependences of this ratio on  $a$  are computed for the point, which is at the distance  $r = 1.8$  Mpc from central point of the void. In the left panel we show the dependences of this ratio on scale factor  $a$  for the models of dark energy with different values of equation of state parameter. One can see that the lines vary in slope and amplitude for different  $a$ . In the central and right panels of Fig. 2 we show how the ratio  $V_m(r)/|\delta_m(r)|$  depends on  $a$  for different values of the dark energy density in the cosmological models with fixed zero spatial curvature ( $\Omega_k = 0$ ) and fixed matter density ( $\Omega_m = 0.3$ ) accordingly. In the case of fixed spatial curvature the lines correlate

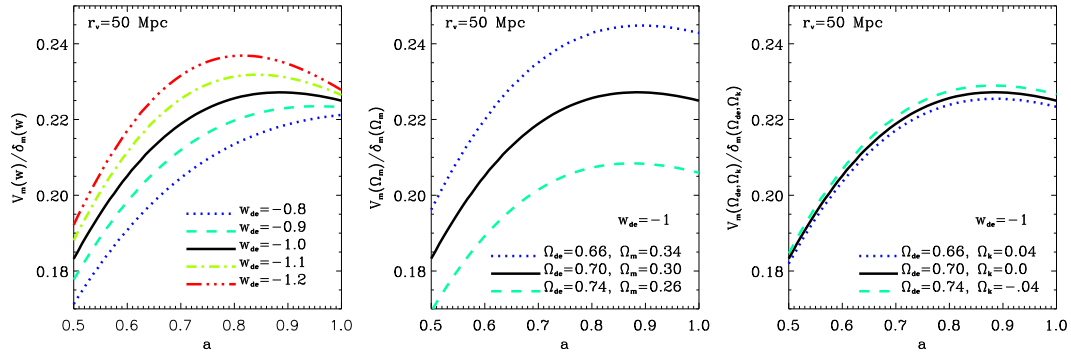


**Figure 2.** The ratio  $V_m/|\delta_m|$  for dark energy models with different values of EoS parameter (left), with different values of density parameter  $\Omega_{de}$  (central) and fixed zero spatial curvature ( $\Omega_k = 0$ ), with different values of density parameter  $\Omega_{de}$  (right) and fixed matter density parameter ( $\Omega_m = 0.3$ ). The dark energy perturbations have not been taken into account.

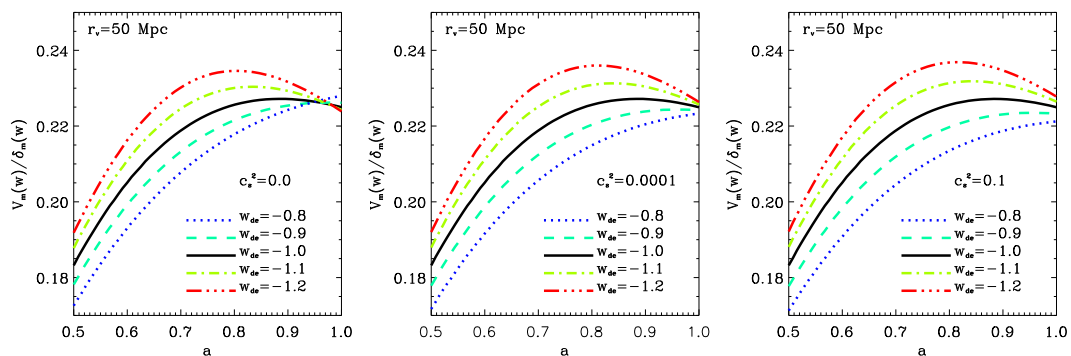


**Figure 3.** The ratio  $V_m/|\delta_m|$  for dynamical dark energy models with different values of effective sound speed. The dark energy perturbations have been taken into account.

with the value of  $\Omega_m$  since the equality  $\Omega_{de} + \Omega_m + \Omega_k = 1$  is always true. The equations (3.5) and (3.7) explain this. When  $\Omega_{de}$  and  $\Omega_k$  are free parameters for fixed  $\Omega_m$  (right panel), the lines vary less, this illustrates the well-known degeneracy between these parameters. Since the Planck 2015 results state that  $|\Omega_k| < 0.005$  [64], the results in the right panel have only the theoretical meaning. Therefore, we can state that the observational data on ratio  $V_m(r)/|\delta_m(r)|$  for the large voids can be used to constrain the values of density and equation of state parameters.

Let us integrate now the system of eqs. (3.5)-(3.7) in the complete version, when the solutions for all functions  $v$ ,  $\delta_m$ ,  $v_m$ ,  $\delta_{de}$ ,  $v_{de}$ ,  $\delta_{rel}$ ,  $v_{rel}$  are sought. The amplitudes of density perturbations of dark energy depend at the late stages of evolution on the value of squared effective sound speed  $c_s^2$  of dark energy, they are larger for lower  $c_s^2$  [20]. The results show that the impact of dark energy perturbations on the matter ones is negligibly small for dark energy models with  $c_s^2 > 0.01$ . It is noticeable only for small values of the effective speed of sound. In Fig. 3 we show the dependences of ratio  $V_m(r)/|\delta_m(r)|$  on  $a$  for  $c_s^2 = 0, 10^{-4}, 0.1$ . One can see that the right plot for  $c_s^2 = 0.1$  does not differ practically from the left plot in Fig. 2, where the perturbations of dark energy have not been taken into account at all. The maximal differences of ratios  $V_m(r)/|\delta_m(r)|$  for the corresponding models in the left panels of Figs. 2 and 3 are within 2-3 percent. So, the high accuracy data of future observations can be used for constraining of  $c_s^2$  from below.

Therefore, the observational data on structure of voids and peculiar velocities of galaxies in them at different redshifts can be used for distinguishing of models of dark energy and determination of their parameters. We understand that these results indicate only the sensitivity of void characteristics to the parameters of dark energy models for the single spherical voids. The most of real voids are non-spherical, surrounded by massive structures, and the galaxies and dark matter are biased. The impact of form of

voids, their surroundings and galactic biasing can be taken into account on the basis of detailed N-body simulations of the formation of large scale structure of the Universe.

## 4. Conclusions

The voids as elements of the large scale structure of the Universe are studied intensively during almost forty years since their discovery. We have learned many interesting things about their origin, formation, properties and population, but many problems connected with them remain unsolved. Huge scientific activity in the world is connected with the dark energy – “the mystery of millennium”, as Thanu Padmanabhan, renowned Indian theoretical physicist and cosmologist, said after publication of the results supporting surely that something like the cosmological constant is inherent for our Universe. Its nature remains unknown despite the tremendous efforts of theoretical physicists, cosmologists and astrophysicists to shed the light into this dark kingdom. Perhaps the combination of efforts in research of these two kinds of “darkness” will help us to understand the nature of both. Presented here results nourish this hope.

## References

1. Einstein A., Sitzungsberichte der Königlich Preussischen Akademie der Wissenschaften (Berlin), 1917, 142.
2. Perlmutter S. et al., *Astrophys. J.*, 1999, **517**, 565; doi:10.1086/307221.
3. Riess A. G. et al., *Astron. J.*, 1998, **116**, 1009; doi:10.1086/300499.
4. Schmidt B. P. et al., *Astrophys. J.*, 1998, **507**, 46; doi:10.1086/306308.
5. Huterer D. & Turner M.S., *Phys. Rev. D*, 1999, **60**, 081301; doi:10.1103/PhysRevD.60.081301.
6. L. Amendola and S. Tsujikawa, *Dark Energy: theory and observations*, Cambridge University Press, 2010, 507 p.
7. G. Wolschin, *Lect. Notes Phys.* 800, 188 (2010); doi:10.1007/978-3-642-10598-2.
8. *Dark Energy: Observational and Theoretical Approaches*, Ed. P. Ruiz-Lapuente, 2010, Cambridge University Press, Cambridge, England, 321 p.
9. B. Novosyadlyj, V. Pelykh, Yu. Shtanov, A. Zhuk, *Dark energy: observational evidence and theoretical models*, eds. V. Shulga, 2013, Akadempriodyka, Ukraine, 381 p.
10. Li B. & Zhao H., 2009, *Phys. Rev. D*, **80**, 044027; doi:10.1103/PhysRevD.80.044027.
11. Biswas R., Alizadeh E. & Wandelt B.D., 2010, *Phys. Rev. D*, **82**, 023002; doi:10.1103/PhysRevD.82.023002.
12. Bos E.G.P., van de Weygaert R., Dolag K. & Pettorino, V., 2012, *MNRAS*, **426**, 440; doi:10.1111/j.1365-2966.2012.21478.x.
13. Li B., Zhao G.-B. & Koyama K., 2012, *MNRAS*, **421**, 3481; doi:10.1111/j.1365-2966.2012.20573.x.
14. Clampitt J., Cai Y.-C. & Li B., 2013, *MNRAS*, **431**, 749; doi:10.1093/mnras/stt219.
15. Jennings E., Li Y. & Hu W., 2013, *MNRAS*, **434**, 2167; doi:10.1093/mnras/stt1169.
16. Cai Y.-C., Padilla N. & Li B., 2015, *MNRAS*, **451**, 1036; doi:10.1093/mnras/stv777.
17. Dai D.-C., 2015, *MNRAS*, **454**, 3590; doi:10.1093/mnras/stv2208.
18. Hamaus N., Sutter P.M., Lavaux G. & Wandelt B.D., 2015, *JCAP*, **11**, 036; doi:10.1088/1475-7516/2015/11/036.
19. Tsizh M., Novosyadlyj B., 2016, *Adv. Astron. Space Phys.*, **6**, 28; doi:10.17721/2227-1481.6.28-33.
20. Novosyadlyj B., Tsizh M., Kulinich Yu., 2017, *MNRAS*, **465**, 482; doi:10.1093/mnras/stw2767.
21. Bond J. R., Kofman L., Pogosyan D., 1996, *Nature*, **380**, 603; doi:10.1038/380603a0.
22. Albert R., Barabasi A. L., 2002, *Rev. Mod. Phys.*, **74**, 47; doi:10.1103/RevModPhys.74.47.
23. Holovatch Yu., Olemskoi O., von Ferber C., Holovatch T., Mryglod O., Olemskoi I., Palchykov V., 2006, *J. Phys. Stud.*, **10**, 247.
24. Holovatch Yu., Kenna R., Thurner S., 2016, arXiv:1610.01002
25. Gregory S.A. & Thompson L.A., *Astrophys. J.*, 1978, **222**, 784; doi:10.1086/156198.
26. Joeveer M., Einasto J. & Tago E., *MNRAS*, 1978, **185**, 357; doi:10.1093/mnras/185.2.357.
27. Zeldovich Ia. B., Einasto J. & Shandarin S. F., *Nature*, 1982, **300**, 407; doi:10.1038/300407a0.
28. Silk J., Szalay A. S. & Zel'dovich Ya. B., *Scientific American*, 1983, **249**(4), 56; doi: 10.1038/scientificamerican1083-72.
29. Sato H., *General relativity and gravitation*, 1984, **A86-12326**, 289.
30. Maeda K., Sasaki M. & Sato H., *Progress of Theoretical Physics*, 1983, **69**, 89; doi:10.1143/PTP.69.89.
31. Fujimoto M., *Astronomical Society of Japan*, 1983, **35**(2), 159.
32. Icke V., *MNRAS*, 1984, **206**, 1; doi:10.1093/mnras/206.1.1P.

33. Ryden B. S. & Turner, E. L., *Astrophysical Journal*, 1984, **287**, L59; doi:10.1086/184398.
34. Vettolani G., de Souza R., Marano B. & Chincarini G., *Astronomy and Astrophysics*, 1985, **144**(2), 506.
35. Mao et al. A Cosmic Void Catalog of SDSS DR12 BOSS Galaxies, submitted to *Astrophys. J.*, 2016, arXiv:1602.02771.
36. Pierre M., Shaver P. A. & Iovino A., *Astronomy and Astrophysics*, 1998, **197**, L3.
37. Ostriker J. P., Bajtlik S. & Duncan R. C., *Astrophysical Journal*, 1988, **327**, L35; doi:10.1086/185135.
38. Dobrzycki A. & Bechtold J., *Astrophysical Journal*, 1991, **377**, L69; doi:10.1086/186119.
39. Stark C.W., Font-Ribera A., White M. & Lee K.-G., submitted to *MNRAS*, 2014, arXiv:1504.03290.
40. Ouchi M., Shimasaku K., Akiyama M., Sekiguchi K. et al., *Astrophys. J.* 2005, **620**, L1; doi:10.1086/428499.
41. Colberg J.M. et al., *MNRAS*, 2005, **360**, 216; doi:10.1111/j.1365-2966.2005.09064.x.
42. Gottlober S., Lokas E. L., Klypin A., & Hoffman Y., *MNRAS*, 2003, **344**(3), 715; doi:10.1046/j.1365-8711.2003.06850.x.
43. Arbabi-Bidgoli S. & Mueller V., *MNRAS*, 2002, **332**, 205; doi:10.1046/j.1365-8711.2002.05296.x.
44. Wojtak R., Powell D. & Abel T., *MNRAS*, 2016, **458**, 4431; doi:10.1093/mnras/stw615.
45. Sutter P. M., Elahi P. & Falck B., *MNRAS*, 2014, **445**, 1235; doi:10.1093/mnras/stu1845.
46. Sutter P. M., Elahi P. & Falck B., *MNRAS*, 2014 **445**(2), 1235; doi:10.1093/mnras/stu1845.
47. van de Weygaert R., *The Zeldovich Universe: Genesis and Growth of the Cosmic Web*, P roceedings of the International Astronomical Union, IAU Symposium, 2016, **308**, 493; doi:10.1017/S1743921316010504.
48. Haque-Copilah S. & Basu D., *Publications of the Astronomical Society of the Pacific*, **106** no. 695, 67; doi:10.1086/133344.
49. Dubinski J. et al, *Astrophysical Journal*, 1993, **410**(2), 458; doi:10.1086/172762.
50. van de Weygaert R. & Sheth R. K., 2003, arXiv:astro-ph/0310914.
51. Sheth R. K. & van de Weygaert R., *MNRAS*, 2004, **350**(2), 517; doi:10.1111/j.1365-2966.2004.07661.x.
52. Ghigna S., Bonometto S., Retzlaff J., Gottloeber S. & Murante G., *Astrophysical Journal*, 1996, **469**, 40; doi:10.1086/177755.
53. Amendola L., Frieman J. & Waga I., *MNRAS*, 1999, **309**(2), 465; doi:10.1046/j.1365-8711.1999.02841.x.
54. Chantavat T., Sawangwit U., Sutter P. M., & Wandelt B. D. *Phys. Rev. D*, 2016 **93**, 043523; doi:10.1103/PhysRevD.93.043523.
55. Krause E., Chang T.-C., Dore O. & Umetsu K., *Astrophysical Journal*, 2013, **762**, L20; doi:10.1088/2041-8205/762/2/L20.
56. Alcock C., Paczynski B., *Nature*, 1979, **281**, 358; doi:10.1038/281358a0.
57. Lavaux G., Wandelt B.D., *Astrophys. J.*, 2012, **754**, 109; doi:10.1088/0004-637X/754/2/109
58. Sutter P. M., Pisani A., Wandelt B.D. & Weinberg D.H., *MNRAS*, 2014, **443**, 2983; doi:10.1093/mnras/stu1392.
59. Neyrinck M., *MNRAS*, 2008, **386**, 2101; doi:10.1111/j.1365-2966.2008.13180.x.
60. Sutter P.M. et al, *Astronomy and Computing*, 2015, **9**, 1.
61. Hamaus N., Sutter P.M. & Wandelt B.D., *Phys. Rev. Lett.*, 2014, **112**, 251302; doi:10.1103/PhysRevLett.112.251302.
62. Nadathur S. et al, 2016, *The Zeldovich Universe: Genesis and Growth of the Cosmic Web*, Proceedings of the International Astronomical Union, IAU Symposium, **308**, 342; doi:10.1017/S1743921316010541.
63. Ricciardelli E., Quilis V. & Varela J. *The Zeldovich Universe: Genesis and Growth of the Cosmic Web*, Proceedings of the International Astronomical Union, IAU Symposium, 2016, **308**, 551; doi:10.1017/S1743921316010565.
64. Planck Collaboration, *Astron. and Astrophys.*, 2016, **594**, A13; doi:10.1051/0004-6361/201525830.
65. Riess A., Macri L. M., Hoffmann S. L. et al., *Astrophys. J.*, 2016, **826**, id. 56; doi:10.3847/0004-637X/826/1/56.
66. Li B., *MNRAS*, 2011, **411** 2615; doi:10.1111/j.1365-2966.2010.17867.
67. Spolyar D., Sahlen M., Silk J., *Phys. Rev. Lett.*, 2013, **111**, 241103; doi:10.1103/PhysRevLett.111.241103.
68. Lavaux G., Wandelt B.D., *MNRAS*, 2010, **403**, 1392; doi:10.1111/j.1365-2966.2010.16197.x.
69. Novosyadlyj B., Tsizh M., Kulinich Yu., 2016, *Gen. Relativ. Grav.*, **48**, 30; doi:10.1007/s10714-016-2031-8.